ISSN 0915-633X

NATIONAL INSTITUTE FOR FUSION SCIENCE

Simulation of Burning Plasma Dynamics in ITER

J.F. Wang, T. Amano, Y. Ogawa, N. Inoue

(Received - Jan. 23, 1996)

NIFS-398 Feb. 1996

RESEARCH REPORT
NIFS Series

NAGOYA, JAPAN

Simulation of Burning Plasma Dynamics in ITER

J.F. Wang, T. Amano, Y. Ogawa †, N. Inoue†

National Institute for Fusion Science

Nagoya 464-01, Japan

† *Faculty of Engineering, The University of Tokyo*

Tokyo 113 , Japan

Abstract

Dynamics of burning plasma for various transient situations in ITER plasma has been simulated with a 1.5-dimensional up-down asymmetry Tokamak Transport Simulation Code (TTSC). We have mainly paid attention to intrinsic plasma transport processes such as the confinement improvement and the change of plasma profiles. It is shown that a large excursion of the fusion power takes place with a small improvement of the plasma confinement; e.g., an increase of the global energy confinement by a factor of 1.22 yields the fusion power excursion of $\sim 30\%$ within a few seconds. Any feedback control of fueling D-T gas is difficult to respond to this short time scale of fusion power transient. The effect of the plasma profile on the fusion power excursion has been studied, by changing the particle transport denoted by the inward pinch

parameter C_V. It is found that the fusion power excursion is mild and slow, and the feedback control is quite effective in suppressing the fusion power excursion and in shortening the duration time of power transient in this case. The change in the pumping efficiency has also been studied and a large excursion of the fusion power has not been observed, because of the decrease in the fuel density itself in the case of the increase in the pumping efficiency, and the helium ash accumulation in the case of the decrease in the pumping efficiency. Finally it is shown that the MHD sawteeth activity leads to the fusion power fluctuation of $\pm$ 20%, although it is helpful for the helium ash exhaust.

Keywords: Burning plasma, ITER, transient dynamics, confinement improvement, plasma profiles, pumping, fueling, Sawteeth.

1 Introduction

The study of burning plasma dynamics is crucial to the successful operation of future fusion reactors such as long pulsed [1] or steady state tokamak reactor [2] and Stellarator reactor [3]. From physical points of view, the dynamics of burning plasma is also very interesting and complicated, since it involves many simultaneous nonlinear processes of transport and reactions. The burning plasma dynamics is governed by the transport equations of plasma density, plasma temperature and current density profiles, including various sources and sinks. More importantly, there is still a lack in understanding of the anomalous particle and energy diffusion behaviour in present fusion devices, and sometimes the diffusion coefficients may be determined by the plasma profiles themselves. Clearly, it is impossible to solve such transport equations exactly by analytical approach. The central expansion techniques [4, 5] has been adopted to study the dynamic properties of burning plasma, where many assumptions have to be made in this procedure. Many authors [6, 7] also modeled the burning plasma dynamics to study the thermal instability of tokamak reactor as well as the feasibility of burn control methods by global model, but such zero dimensional approach does not adequately describe the radial profile and diffusion effects in the burning plasma dynamics. A 1.5 dimensional modeling approach such as PRETOR [8] code, has recently been adopted to address the dynamics of burning plasma in ITER, in which a hypothetical sudden improvement in confinement mode was considered.

Since various transient situations can produce an unanticipated power transient which yields the increase in power loading on the in-vessel components, it is worthwhile to evaluate the power excursion level quantitatively in the magnitude and the duration. The thermal

runaway of the fusion power is one of the most important issues, and typical accidental events triggered by wrong operation of external systems, such as injection of excess fueling gas. In addition to the fusion power excursion due to the external causes, internal causes triggered by plasma performance should be considered in the burn control scenario and designing the safety system.

The motivation of this work is to make a thorough understanding of the plasma responses to various transient situations, mainly due to intrinsic transport processes perturbations and extrinsic operational changes. In view of the uncertainty of intrinsic transport processes, such as anomalous particle and energy diffusion in present experiments, we refer intrinsic transport processes changes as the hypothetical sudden increase in plasma confinement characteristics, such as L- to H-mode/H- to VH-mode transitions, and as the sudden changes in plasma profiles caused by MHD perturbation like big ELM's and sawteeth. On the other hand, particle balance in burning plasmas is governed by the fueling and pumping capacity, we consider the changes in pumping and fueling efficiency as extrinsic operational changes. In this paper, we mainly concentrate on the physical consequences of the transient dynamics behaviour in ITER and are expecting that these simulation results will give fruitful information on the magnitude and the response time of the fusion power excursion for designing feedback scenario and safety system.

In section 2, a brief description of physics models is presented, and in section 3 the simulation results on the transient dynamics of ITER burning plasma are discussed, and finally summary and conclusions are given in section 4.

2 Physics Models

A 1.5-dimensional up-down asymmetry Tokamak Transport Simulation Code (TTSC), which consistently couple a 2-dimensional up-down asymmetry equilibrium solver with a 1-dimensional flux surface averaged transport solver, is developed and used to predict the various transient plasma performance for ITER design. The plasma particles are treated as three species (deuterons, triton and helium ions), and impurities are included as specified fraction of D-T ions, while electron density is calculated from the charge neutrality condition. Electron and ion temperatures are solved through transport equations separately, although it is assumed that all ions have the same temperature. Plasma D-T fuel is provided by gas-puffing and/or pellet injection, and plasma exhaust is modeled through specified recycling rate R at the edge in present study. The D-T fueling rate can be controlled for two purposes; one is the fusion power feedback scheme where the fueling rate is controlled so as to keep the fusion power at the specified value, and the another is the density feedback scheme where the volume-average electron density is controlled at the prescribed value. Burn control through auxiliary heating power is also implemented. Sawteeth events are simulated through enhanced transport in the inverse radius region or by flattening the plasma profiles when disruptions occur (Kadomtsev-like model). Sawteeth period is derived from the Park-Monticello scaling [9] or specified.

Accurate prediction of plasma performance depends on the transport model, however, theoretical models describing the anomalous transport are still incomplete or do not fit the experimental data well. It is claimed that our present lack of knowledge of transport does not prevent us from making good prediction of plasma performance of a fusion reactor by

means of dimensionally similar discharge experiments [10]. Recent experimental results in TFTR [11] and JET [12] indicate that transport model of Bohm type allows a good representation of experimental data fit. A simple transport coefficients of the Bohm type has been proposed on the basis of the JET discharge data, which has shown that many results of JET L-mode discharge can be simulated very well with this model [13]. This model was adopted for simulation of ITER plasma in this paper.

In plasma transport model, the transport coefficients come from neoclassical transport contribution and anomalous transport contribution, We assume the anomalous electron and ion heat diffusivity as

$$\chi_{\rm e} = \chi_{\rm i} = \chi_{\rm Bohm}/f_{\rm ch} \ , \tag{1}$$

Here $\chi_{\rm Bohm}$ is the Bohm type transport coefficient based on JET data [13], given by

$$\chi_{\rm Bohm} = C_{\rm B}\frac{\nabla(n_{\rm e}T_{\rm e})}{n_{\rm e}B_{\rm t}}q^2 \ , \tag{2}$$

where $C_{\rm B} = 3.3 \times 10^{-4}$ (SI units and $T_{\rm e}$ in eV), $B_{\rm t}$ denotes the toroidal field strength in Teslar and q is the safety factor. To simulate the improved confinement plasmas, we introduce an improved-confinement factor $f_{\rm ch}$ by which the heat diffusivity is reduced. We note that this factor f_{ch} adopted here is corresponding to the enhancement factor of the energy confinement time (so-called H factor) with the relation of H-factor $= \sqrt{f_{ch}}$.

The particle transport is assumed to be

$$D = \chi_{\rm e}/3, \qquad V_{\rm pinch} = -C_{\rm V}\frac{2r}{a^2}D \ , \tag{3}$$

where $V_{\rm pinch}$ is the particle inward pinch velocity defined with a inward pinch parameter $C_{\rm V}$.

3 Simulation of Plasma Transient Dynamics

In this section, we discuss the simulation results of transient dynamics on burning plasma in ITER EDA, by using the models described in the previous section. The ITER EDA plasma parameters are listed in Table 1 [14]. The ITER EDA plasma configuration calculated is shown in Figure 1. We start from simulation of the ITER EDA reference plasma with 1.5 GW fusion power, and the perturbations are initiated at the steady state phase. Since many physical phenomena affect on the plasma parameters, yielding the fusion power excursion, it is worthwhile to identify a dominant factor in plasma property quantitatively.

First we consider the intrinsic transport processes, which is caused by the sudden improvement in energy confinement, modeled by the increase in improved-confinement factor f_{ch}, and the sudden changes in particle transport, modeled by the change in the inward pinch parameter C_V. Next we consider the extrinsic operational changes, such as the sudden change in pumping efficiency, modeled with the change in recycling coefficient R, and sudden change in fueling system capability, modeled by fueling rate change. Finally, the effects of MHD perturbation of sawteeth on fusion power excursion are investigated.

3.1 Effects of Confinement improvement

In this study, we refer the perturbation with period of several to several tens seconds as temporary perturbation, and the perturbation with period of more than several hundred seconds as permanent perturbation. The perturbations are introduced by the procedure

that all local transport coefficients are instantaneously decreased over the entire plasma radius (the increase of the improved-confinement factor of fch). This instantaneous reduction of local transport coefficients over the wide plasma region has been observed experimentally in the L-H transition on JET [15] and JT60U [16]. Numerical analysis [17] supports this instantaneous improvement on the thermal diffusivity.

Usually some feedback control system or the fusion power might be anticipated in fusion reactor, and feedback control schemes are implemented in TTSC code. However, to simulate a worse situation of the fusion power excursion, we have considered the condition of the constant gas fueling first. Figure 2 shows the transient behaviors of the fusion power for various perturbation periods in the case of constant fueling, where the improved-confinement factor f_{ch} of the thermal diffusivity is changed from 4.0 ($\tau_E = 3.74s$) to 6.0 ($\tau_E = 4.68s$) at $t = 49$ seconds. This is corresponding to the improvement of global energy confinement time by a factor of $\sqrt{6.0/4.0} \simeq 1.22$ according to the derived thermal confinement scaling [13]. We see that for perturbation with period of 1 second, the power excursion is about 5% of the normal operation power, and the duration of the transient is about 10 seconds. The power excursion increases with the prolongation of the perturbation period, and saturates with perturbation period longer than 10 seconds due to the effects of helium ash accumulation. Even for permanent perturbation, the power excursion is about 30%, and the characteristic duration of the transient is about 50 seconds. This time is essentially corresponding to the characteristic time of helium accumulation.

Figure 3 shows the excursion of fusion power, helium fraction, plasma temperature, and plasma density for several improvements in confinement in the case of constant fueling and

permanent perturbations. We see that large improvement of the confinement (large f_{ch} value) enlarges the power excursion value, but does not change the characteristic duration of the transient. This is because that the improvement in confinement does not affect the time scale of helium accumulation, although it may result in larger helium fraction value.

We can also say that even when the plasma confinement is extremely improved such as the case of $f_{ch} = 16$, the thermal runaway of the fusion power does not take place, because of the helium ash accumulation, although the excursion level of the fusion power becomes quite large (e.g., the maximum fusion power $P_{fus} \sim 3$ GW at $f_{ch} = 16$). In addition, the duration of the fusion power excursion is at most ~ 50 seconds, as shown in Fig. 3.

The maximum fusion power is plotted in Fig. 4 as a function the improved-confinement factor normalized by that of the initial steady state. If the maximum level of the fusion power is limited at a specified value by the safety reasons, the allowable level of the confinement improvement is restricted within a very narrow window on the confinement improvement; for example, if the maximum fusion power is limited to be 1.8 GW, the improved-confinement factor f_{ch} should be less than 5.25, which requires the control of the global confinement time within a factor of 1.15.

In Fig. 4, the response times to reach the fusion power to the specified limit value are also plotted, where two cases on the power excursion of 20% ($P_{fus} = 1.8$ GW) and 50% ($P_{fus} = 2.25$ GW) are presented. The response time is typically less than 10 seconds, which is roughly corresponding to the energy confinement time, and weakly dependent on the improved-confinement factor. If the maximum fusion power must be restricted within

some specified value, We need some feedback scenario within this response time.

Next we have considered the feedback scenario by controlling the gas fueling rate so as to reduce the power excursion as low as possible. Figure 5 shows temporal evolutions of the fusion power, helium ash, plasma temperature and density for three cases; i.e., constant fueling, fusion power feedback control and density feedback control. The gas-feed rate is set to be zero during the short period just after the switch-on of the confinement improvement, and it is difficult to suppress the increase in the fusion power at this initial phase. Nevertheless, the maximum level of the fusion power excursions are reduced by $\sim$ 15% for fusion power feedback control and $\sim$ 10% for density feedback controls, respectively. Durations are also remarkably shortened to 15 seconds and 30 seconds, respectively.

Since the response time at the initial phase does not change so much even by the introduction of gas-feedback control, some safety scenario should be anticipated during this short period for the burning control, if the excess of the fusion power must be strictly limited at the specified value.

3.2 Effects of plasma profile changes

The changes of plasma profiles are modeled with instantaneous perturbations of the inward pinch parameter C_V, where larger C_V value yields the more peaked density profile.

The effect of plasma profile perturbation on power excursion is shown in Fig. 6, which reveals the important role of plasma profiles in burning plasma performance and dynamics behaviour. We find that sudden peaking plasma profiles with the inward pinch parameter C_V from 1.0 ($n_0/ < n >= 1.6$) to 2.0 ($n_0/ < n >= 3.0$) leads to very large increase of

fusion power by a factor of $3 \sim 4$, and does not return to their original level. In the case of $C_V = 1.5$, the fusion power excursion of 40% occurs when no feedback control, and the characteristic time to reach the 20% fusion power excursion is 6 seconds, which is relatively longer than those in the cases of the confinement improvement shown in Fig. 4. In Fig. 6, the simulation with feedback control is also plotted in the case of $C_V = 1.5$, where the power excursion is remarkably suppressed and the duration of the power excursion is shortened. We can, therefore, say that the fusion power excursion might be suppressed below 1.8 GW (20% excursion) by the feedback control of the fueling gas, when the change in C_V value from $C_V = 1.0$ is less than 1.5.

3.3 Effects of pumping efficiency perturbation

The effect of the pumping efficiency is modeled by changing the recycling coefficients R . In order to understand the role of the pumping system efficiency for D-T fuel and helium, we compared two cases in Fig. 7. In the case of Fig. 7 (a), only the recycling rate for the helium is changed, keeping the recycling rate of D-T fuel to be unchanged, and in the case of Fig. 7 (b), the recycling rates for both D-T fuel and helium are changed. It is shown that no ignition can be sustained in both Fig. 7(a) and Fig. 7(b) for the recycling coefficients of 0.998 because of excessive helium accumulation. In the former case, since the amount of D-T fuel does not change with helium pumping efficiency perturbation, the decrease in recycling coefficients R_{He} would lead to the decrease in electron density and radiation power (Bremsstrahlung), yielding the increase in plasma temperature and alpha heating power. In the latter case, the decrease in recycling coefficients yields the reduction in the

D-T fuel itself, in addition to the decrease in the electron density and Bremsstrahlung radiation losses and the increase in the temperature, resulting in no increase in the fusion power, as shown in Fig. 7 (b).

The remarkable excursion of the fusion power can be seen when the recycling rate is decreased only for the helium, as shown in Fig. 7 (a). With no feedback control, the maximum excursion of the fusion power is at most 1.8 GW, and it takes about 25 seconds. These excursions of the fusion power seem to be acceptable in designing safety scenario.

3.4 Effects of fueling rate change

The fueling system capability change is simulated with the increase in fueling rate of the D-T fuel. Figure 8 (a) shows the fusion power for the various fueling rate (10%, 20% and 30% increase), and the fusion power saturates at an elevated level (9%, 18% and 27%, respectively). If the particle confinement time is assumed to be constant, the plasma density is proportional to the fueling rate, yielding the increase in the fusion power proportional to the square of the fueling rate. However, as shown in Fig. 8, the fusion power is not proportional to the square of the fueling rate because of the change of temperature, it is also because the increase in the fusion power degrades the particle confinement, resulting in suppressing the sufficient increase of the density; i.e., the increases in the $< n_e >$ are 3%, 6% and 9% for 10%, 20% and 30% increase in the fueling rate, respectively.

We also studied the role of D-T fuel profiles in the effects of fueling rate change, as shown in Fig. 8 (b), in which the increase in fueling rate is set to be 30% and perturbation is permanent. We find that the fusion power excursions differ for the D-T fuel profiles with

inward pinch parameters of 1.0 and 0.2 respectively, for the same helium profile peaking parameter. This implies that fusion power excursion level is mainly determined by the D-T fuel profiles for the fueling rate perturbation.

3.5 Effects of Sawteeth perturbation

The effects of MHD perturbation on burning plasma dynamics is also an important issue. Here we investigate the effects of sawteeth with the Kadomtsev-like model, where the plasma profiles are flattened when disruptions occur. The sawteeth period is prescribed to 50 seconds. The inversion radius is estimated to be at 1.8m, which is 60% of the plasma minor radius. The sawteeth yield the large oscillation of the fusion power, as shown in Fig. 9 (a), where maximum and minimum fusion powers are 1.8 GW and 1.2 GW, respectively. The sawteeth has advantage of the helium ash exhaust. Figure 9 (b) show the helium fraction, where the sawteeth help the removal of helium ash from the core and the helium fraction is reduced to be 16%.

4 Summary and Conclusions

The dynamics of burning plasma in ITER has been studied with 1.5-D up-down asymmetry Tokamak Transport Simulation Code (TTSC), taking into account the effects of possible intrinsic transport processes changes and extrinsic operation system perturbations. We have considered two cases of intrinsic transport process changes in this study, i.e., the sudden improvement of plasma confinement mode and sudden changes of plasma profiles,

which have been observed in present plasma experiments. Possible consequences of such intrinsic changes of transport processes were simulated on ITER EDA burning plasma with the improved Bohm type transport model.

The large excursion of the fusion power takes place with the small improvement of the plasma confinement : e.g., the increase in the global energy confinement by a factor of 1.22 (i.e., the increase in f_{ch} value from 4 to 6) yields the fusion power excursion of $\sim$ 30%. However, the thermal runaway of the fusion power does not take place due to the helium ash accumulation, and the excursion of the fusion power is a transient phenomenon, and is lasting during the effective particle confinement time of the helium ash. From the viewpoint of safety operation another important point is the response time to reach the fusion power to the specified level. Just after the perturbation of the confinement improvement, the fusion power begins to increase very quickly with a time constant of a few seconds. Even if the feedback control of the fusion power by means of the fuel D-T gas control is introduced, it is difficult to suppress this fast time response. Therefore, a careful control of the energy confinement property should be considered from the viewpoint of the fusion power control.

The effect of the plasma profile change on the fusion power has been studied, by changing the particle transport denoted by the inward pinch parameter C_V. When the C_V value is increased from 1.0 to 1.5, the fusion power excursion reaches 40% with no feedback control, and the response time to reach the fusion power of 20% excursion is 6 seconds. The response time is relatively longer than that in the cases of the confinement improvement, and the feedback control is quite effective in suppressing the fusion power excursion and in

shortening the duration of power transient in this case.

Extrinsic operational changes in pumping and fueling systems are also considered. In general, a sudden change in the pumping efficiency does not yield the large excursion of the fusion power. When the pumping efficiency (the recycling coefficient R_{DT}, R_{He}) is increased for all ions species, the fusion power begins to decrease due to the decrease of the plasma density at the constant fueling rate. When the pumping efficiency is decreased, a slight increase of the fusion power is seen just after the change in the pumping efficiency, and then the ignition quenches due to the excess accumulation of the helium ash. When the pumping efficiency for helium is increased but the pumping efficiency for D-T fuel does not change, the large excursion of the fusion power is observed. The maximum fusion power is 1.8 GW and the response time is a few tens seconds in the case of the change in R_{He} from 0.98 to 0.90.

The increase in the fueling rate yields the increase in the fusion power with a response time of a few tens seconds; e.g., the increase in the fueling rate by 30% leads to the increase of the fusion power by $\sim$ 27%, and the fusion power is not proportional to the square of the fueling rate because of the change of temperature and degradation of the particle confinement time at an elevated fusion power. Also, it was shown that the fusion power excursion level is mainly determined by the D-T fuel profiles for the fueling rate perturbation.

Finally the MHD sawteeth activity leads to the fusion power fluctuation of $\pm$20%, although it is helpful for the helium ash exhaust.

In conclusion, we have shown that possible changes in confinement, plasma profile,

pumping and fueling system efficiencies lead to large fusion power excursion. Especially the plasma confinement change yield the fast response on the fusion power excursion within a few seconds, and any feedback control scenario seems to be difficult. While, for other plasma perturbations, appropriate feedback schemes are quite effective in reducing the fusion power excursion and in shortening the duration of the excess fusion power. It is revealed that understanding of plasma transport mechanism and control of plasma confinement mode and plasma profiles, as well as control of pumping and fueling systems will play an important role in the operation of future fusion reactor. Feedback scenario and safety system should be designed in taking these plasma characteristics into account.

Acknowledgments

One of the authors (J.F. Wang) would like to acknowledge Prof. Z. Yoshida, and Prof. M. Okamoto for encouragement and support during this work, and Dr. T. Tsunematsu for suggestion of topics and fruitful discussions, and also wish to thank National Institute for Fusion Science COE project for financial support.

References

[1] N. Inoue et al., Plasma Phys. and Controlled Nucl. Fusion Res., Würzburg, 1992 (IAEA, Vienna, 1993), Vol.3, p.347.

[2] Y. Seki et al. , Plasma Physics and Controlled Nuclear Fusion Research 1991, Vol. 1, Vienna, IAEA, pp. 473–485 (1991). (Proc. 13th Int. Conf. Washington, 1990).

[3] S.L. Painter and J.F. Lyon, Nucl. Fusion **23** (1991) 2271.

[4] H. Wilhelmsson and M.-N. LeRoux, Physica Scripta **48** (1993) 735.

[5] M.-N. LeRoux and H. Wilhelmsson, Physica Scripta **50** (1994) 705.

[6] S.K. Ho and M.E. Fenstermacher, Fusion Techol. **16** (1989) 185.

[7] J. Mandrekas and W.M. Stacey, Jr., Fusion Techol. **19** (1991) 57.

[8] The ITER Director, Detail of the ITER Outline Design Report, Vol.1(1994) (Proc. 4th. Meeting of the Technical Advisory Committee, San Diego Joint Work Site, 1994).

[9] W. Park and D. Monticello, Nucl. Fusion **32** (1992) 2217.

[10] R.E. Waltz, J.C. Deboo and M.N. Rosenbluth, Phys. Rev. Lett. **65**(1991) 2390.

[11] F.W. Perkins et al, Phys. Fluids B **5**(1993) 477.

[12] J.P. Christiansen et al, Nucl. Fusion **33**(1993) 863.

[13] A. Taroni et al., Plasma Phys. Control. Fusion **36** (1994) 1629.

[14] P-H. Rebut et al., The ITER EDA Outline Design, 15th Int. Conf. on Plasma Physics and Controlled Nuclear Fusion Research, Seville 1994.

[15] S.V.Neudachin et al., in Controlled Fusion and Plasma Physics (Pro. 20th Eur. Conf. Lisbon, 1993), Vol. 17C, Part I, European Physical Society, Geneva(1993) 103.

[16] S.V.Neudachin et al., JAERI-Research 95-060 (1995).

[17] J.G. Cordey et al., Nucl. Fusion **35**(1995) 107.

Figure Captions

Fig.1. ITER EDA plasma equilibrium configuration.

Fig.2. Fusion power excursion for different perturbation period in the case of constant fueling, when the improved-confinement factor f_{ch} is changed from 4.0 to 6.0.

Fig.3. Excursions of (a) Fusion power, (b) helium fraction, (c) temperature and (d) density for different improvement in confinement in the case of constant fueling and permanent perturbation.

Fig.4. The maximum fusion power and the response time to reach 20% and 50% fusion power excursion as a function of the improved-confinement factor f_{ch} and H-factor.

Fig.5. Excursions of (a) Fusion power, (b) helium fraction, (c) temperature and (d) density for constant fueling, with fusion power feedback control and with density feedback control in the case of permanent perturbation, where the improved-confinement factor f_{ch} is changed from 4.0 to 9.0.

Fig.6. Fusion power excursions for different inward pinch parameters C_V in the case of constant fueling and permanent perturbations.

Fig.7. Fusion power excursions for different pumping efficiency in the case of constant fueling, (a) R_{DT}=0.98 and R_{He} is changed and (b) R_{DT}=R_{He} are both changed.

Fig.8. Fusion power excursions (a) for various fueling perturbation (b) and for 30% fueling perturbation with different inward pinch parameter C_V.

Fig.9. Excursions of fusion power and helium fraction with sawteeth and without sawteeth.

Table 1: ITER EDA device major parameters

Major Radius R	8.14 m
Minor Radius a	3.0 m
Plasma configuration	Single-null divertor
Elongation κ_{95}	1.6
Triangularity δ_{95}	0.24
Plasma Current I_{p}	24 MA
Toroidal Field B_{t}	5.68 T
Safety Factor q_{95}	3.0
Fusion Power P_{fus}	1.5 GW

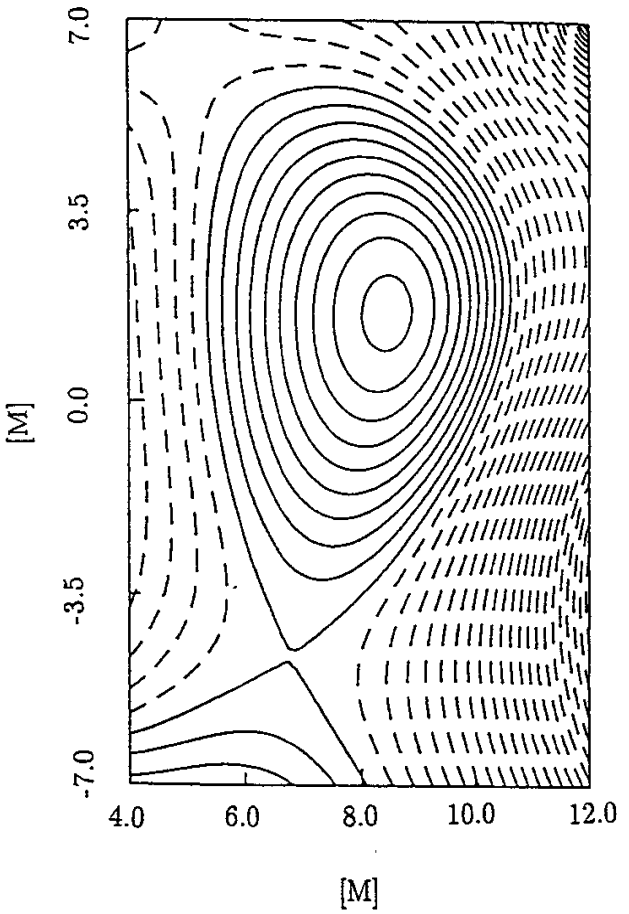

Figure 1:

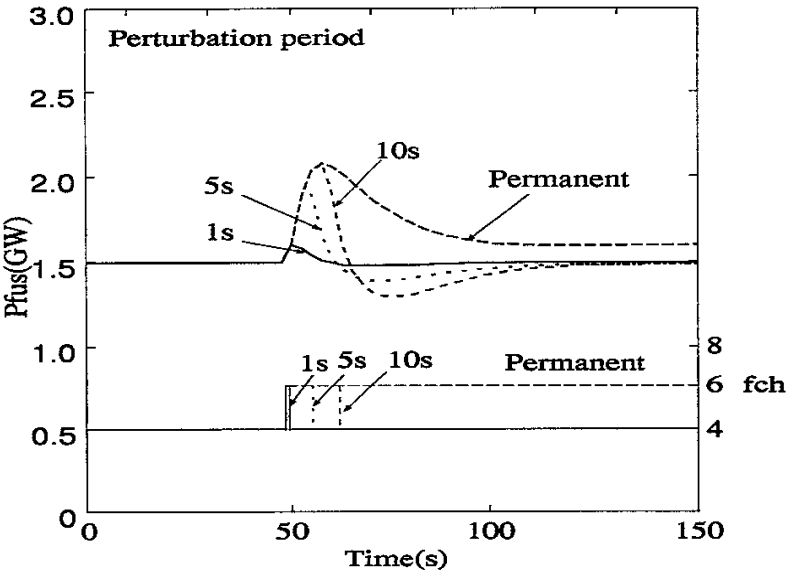
Perturbation period
10s
5s
Permanent
1s
1s 5s 10s
Permanent
fch
Pfus(GW)
Time(s)
3.0
2.5
2.0
1.5
1.0
0.5
0
0
50
100
150
8
6
4

Figure 2:

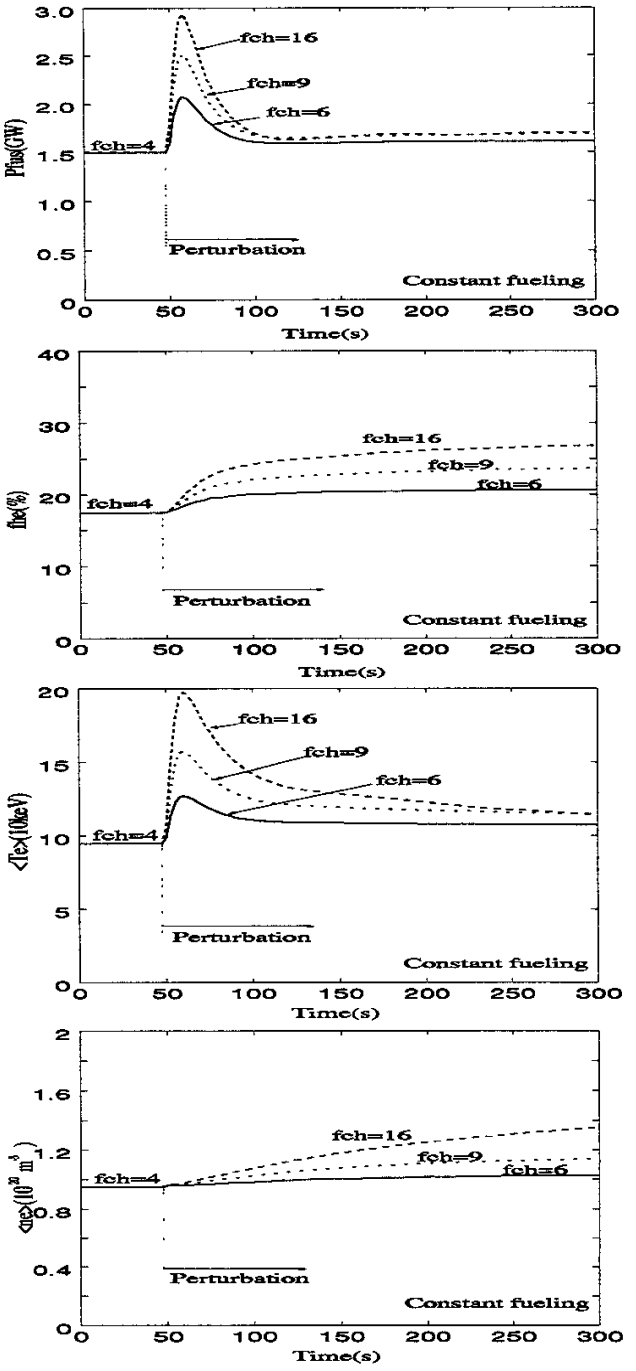
Pfus(GW)
fch=16
fch=9
fch=6
fch=4
Perturbation
Constant fueling
Time(s)
fhe(%)
fch=16
fch=9
fch=6
fch=4
Perturbation
Constant fueling
Time(s)
<Te>(10keV)
fch=16
fch=9
fch=6
fch=4
Perturbation
Constant fueling
Time(s)
<ne>(10^20 m^-3)
fch=16
fch=9
fch=6
fch=4
Perturbation
Constant fueling
Time(s)

Figure 3:

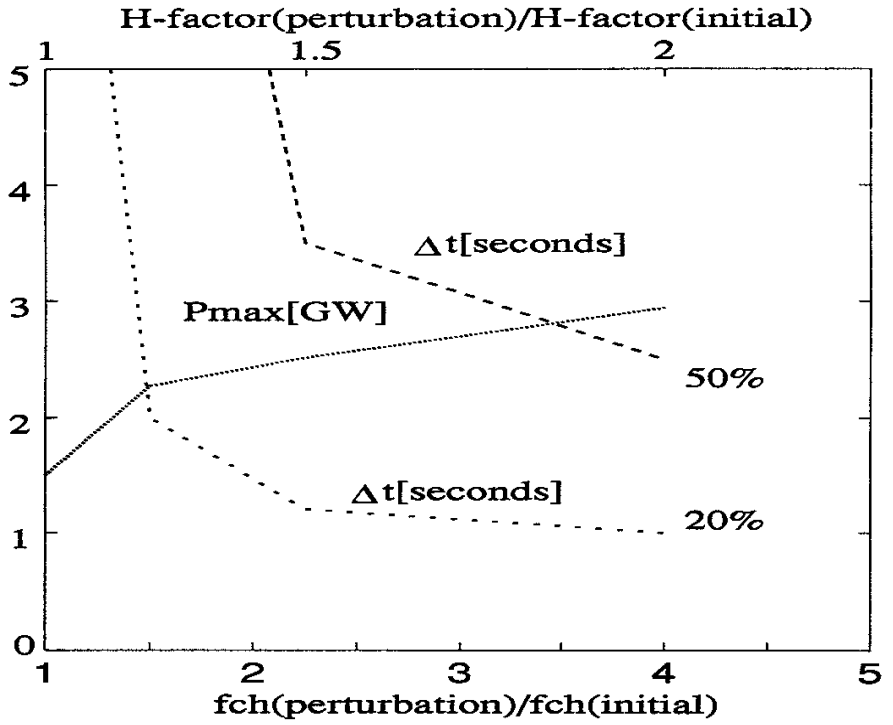
H-factor(perturbation)/H-factor(initial)
1
1.5
2
5
4
3
2
1
0
Δt[seconds]
Pmax[GW]
50%
Δt[seconds]
20%
1
2
3
4
5
fch(perturbation)/fch(initial)

Figure 4:

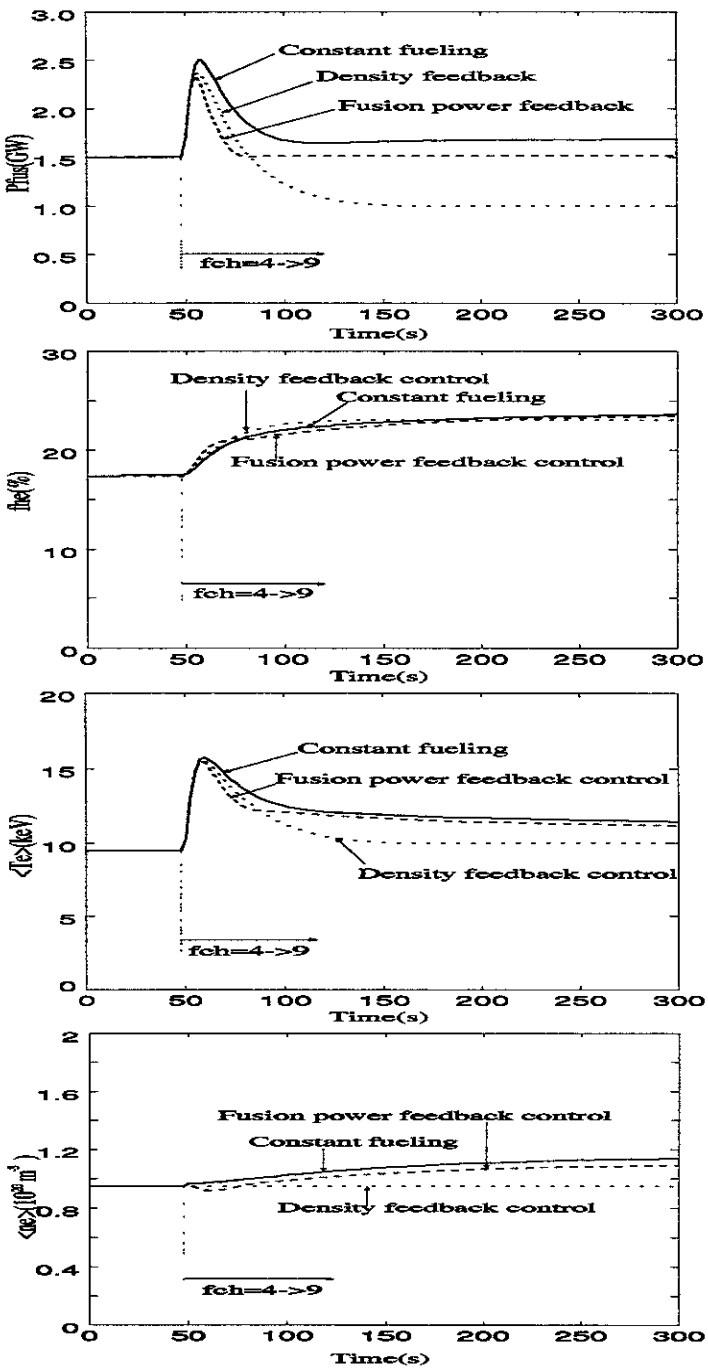
Constant fueling
Density feedback
Fusion power feedback
fch=4->9
Pfus(GW)
Time(s)
Density feedback control
Constant fueling
Fusion power feedback control
fch=4->9
fhe(%)
Time(s)
Constant fueling
Fusion power feedback control
Density feedback control
fch=4->9
<Te>(keV)
Time(s)
Fusion power feedback control
Constant fueling
Density feedback control
fch=4->9
Time(s)

Figure 5:

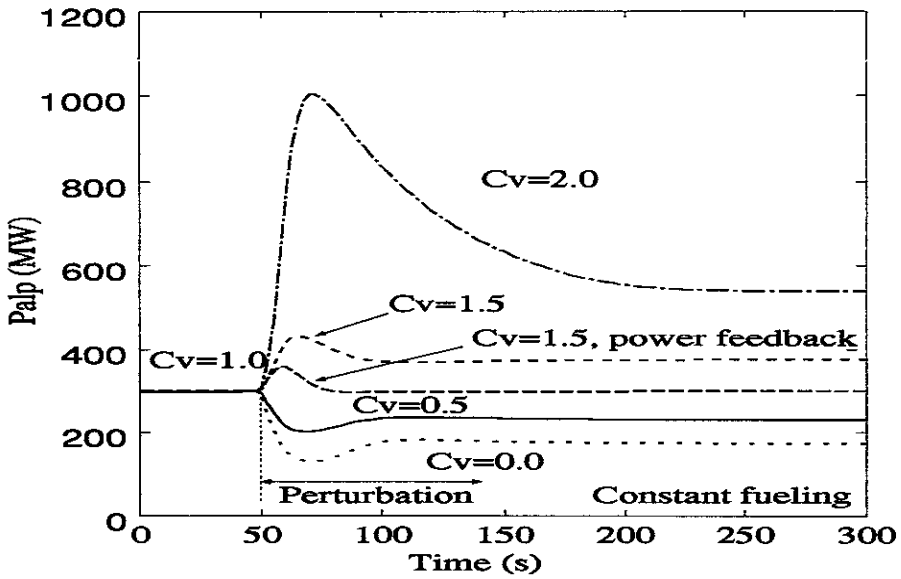
1200
1000
800
600
400
200
0
Palp (MW)
0
50
100
150
200
250
300
Time (s)
Cv=2.0
Cv=1.5
Cv=1.5, power feedback
Cv=1.0
Cv=0.5
Cv=0.0
Perturbation
Constant fueling

Figure 6:

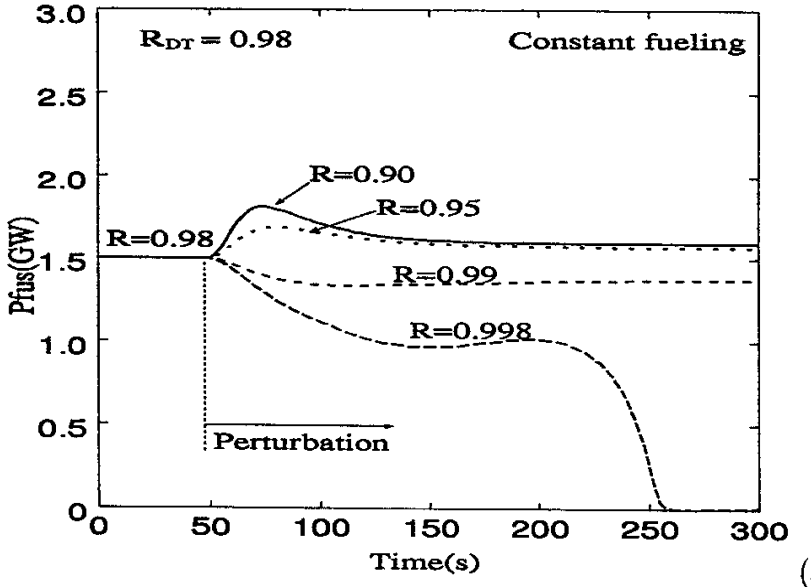
R_{DT} = 0.98
Constant fueling
R=0.90
R=0.95
R=0.98
R=0.99
R=0.998
Perturbation
Pfus(GW)
Time(s)
3.0
2.5
2.0
1.5
1.0
0.5
0
0
50
100
150
200
250
300

(a)

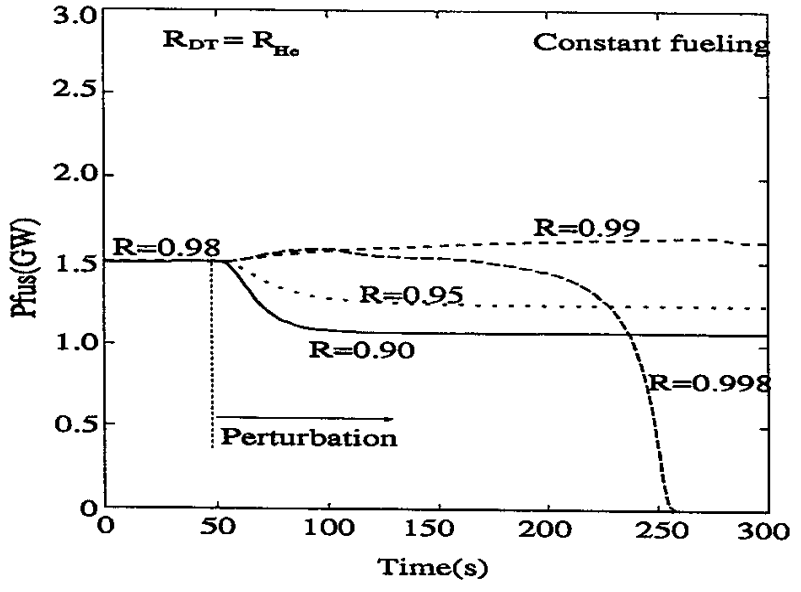
$R_{DT} = R_{He}$
Constant fueling
R=0.99
R=0.98
R=0.95
R=0.90
R=0.998
Perturbation
Pfus(GW)
Time(s)
3.0
2.5
2.0
1.5
1.0
0.5
0
0
50
100
150
200
250
300

(b)

Figure 7:

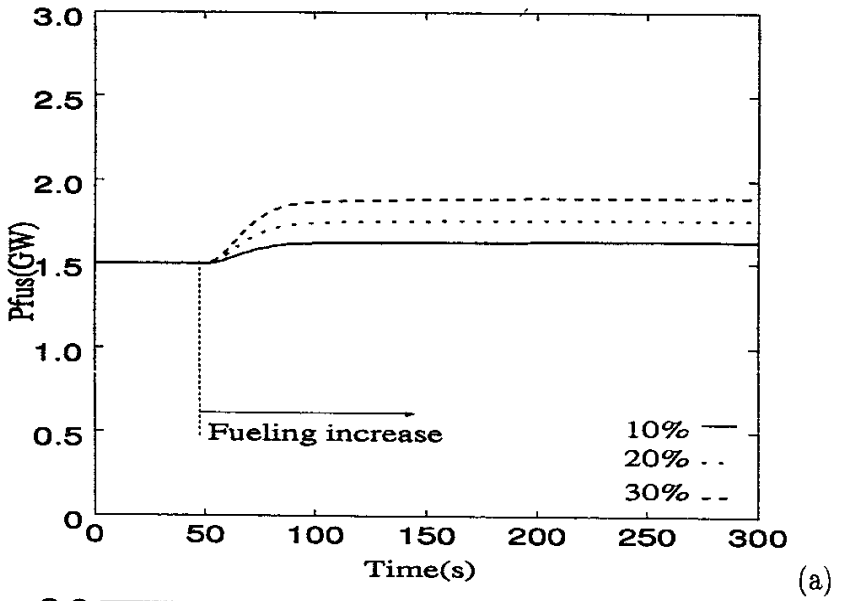
3.0
2.5
2.0
1.5
1.0
0.5
0
Pfus(GW)
Fueling increase
10%
20%
30%
0
50
100
150
200
250
300
Time(s)

(a)

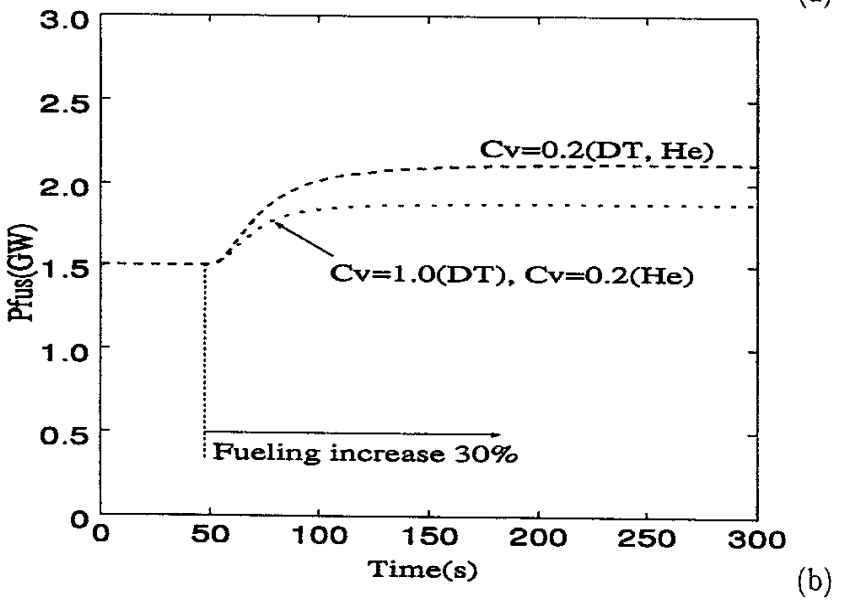
3.0
2.5
2.0
1.5
1.0
0.5
0
Pfus(GW)
Cv=0.2(DT, He)
Cv=1.0(DT), Cv=0.2(He)
Fueling increase 30%
0
50
100
150
200
250
300
Time(s)

(b)

Figure 8:

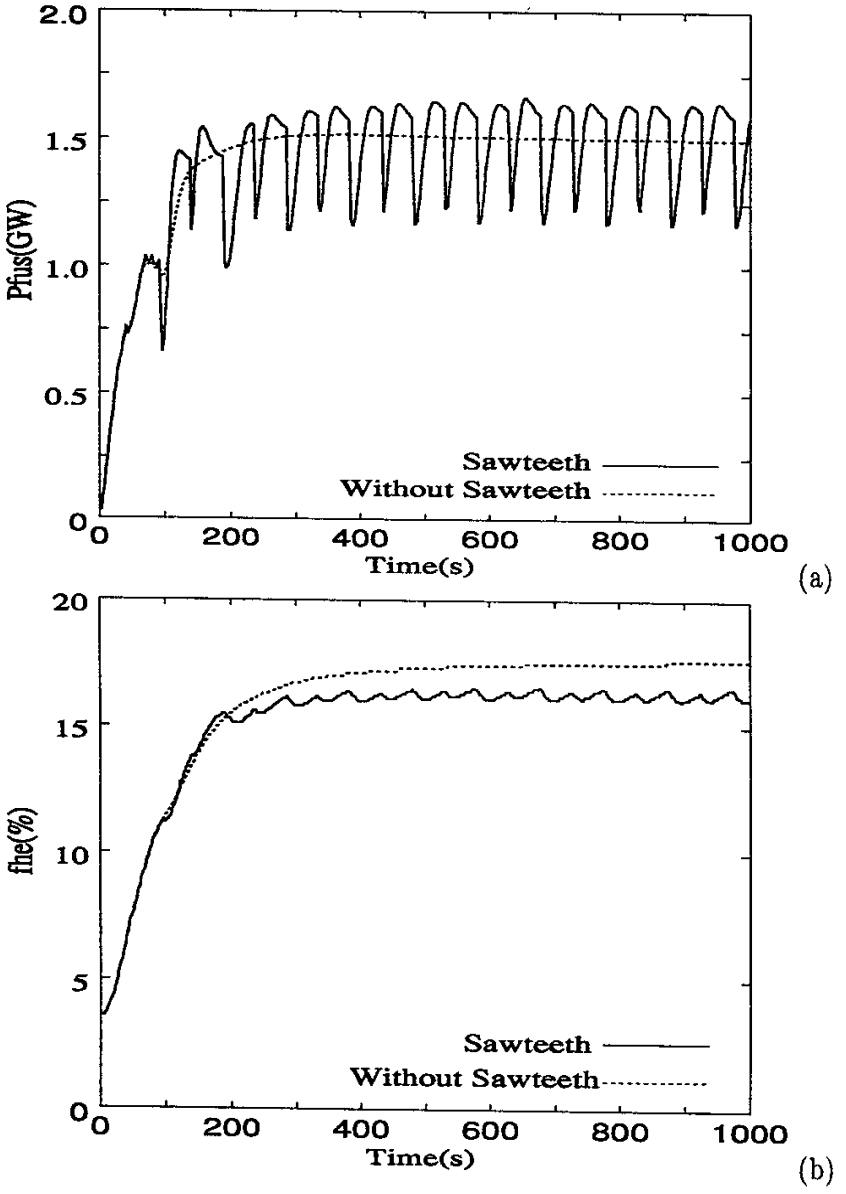
2.0
1.5
1.0
0.5
0
Pfus(GW)
0
200
400
600
800
1000
Time(s)
Sawteeth
Without Sawteeth
(a)
20
15
10
5
0
fhe(%)
0
200
400
600
800
1000
Time(s)
Sawteeth
Without Sawteeth
(b)

Figure 9:

Recent Issues of NIFS Series

NIFS-352 A. Taniike,
Energy Loss Mechanism of a Gold Ion Beam on a Tandem Acceleration System: May 1995

NIFS-353 A. Nishizawa, Y. Hamada, Y. Kawasumi and H. Iguchi,
Increase of Lifetime of Thallium Zeolite Ion Source for Single-Ended Accelerator: May 1995

NIFS-354 S. Murakami, N. Nakajima, S. Okamura and M. Okamoto,
Orbital Aspects of Reachable β Value in NBI Heated Heliotron/Torsatrons; May 1995

NIFS-355 H. Sugama and W. Horton,
Neoclassical and Anomalous Transport in Axisymmetric Toroidal Plasmas with Electrostatic Turbulence; May 1995

NIFS-356 N. Ohyabu
A New Boundary Control Scheme for Simultaneous Achievement of H-mode and Radiative Cooling (SHC Boundary); May 1995

NIFS-357 Y. Hamada, K.N. Sato, H. Sakakita, A. Nishizawa, Y. Kawasumi, R. Liang, K. Kawahata, A. Ejiri, K. Toi, K. Narihara, K. Sato, T. Seki, H. Iguchi, A. Fujisawa, K. Adachi, S. Hidekuma, S. Hirokura, K. Ida, M. Kojima, J. Koong, R. Kumazawa, H. Kuramoto, T. Minami,. M. Sasao, T. Tsuzuki, J.Xu, I. Yamada, and T. Watari,
Large Potential Change Induced by Pellet Injection in JIPP T-IIU Tokamak Plasmas; May 1995

NIFS-358 M. Ida and T. Yabe,
Implicit CIP (Cubic-Interpolated Propagation) Method in One Dimension; May 1995

NIFS-359 A. Kageyama, T. Sato and The Complexity Simulation Group,
Computer Has Solved A Historical Puzzle: Generation of Earth's Dipole Field; June 1995

NIFS-360 K. Itoh, S.-I. Itoh, M. Yagi and A. Fukuyama,
Dynamic Structure in Self-Sustained Turbulence; June 1995

NIFS-361 K. Kamada, H. Kinoshita and H. Takahashi,
Anomalous Heat Evolution of Deuteron Implanted Al on Electron Bombardment; June 1995

NIFS-362 V.D. Pustovitov,
Suppression of Pfirsch-schlüter Current by Vertical Magnetic Field in Stellarators; June 1995

NIFS-363 A. Ida, H. Sanuki and J. Todoroki
An Extended K-dV Equation for Nonlinear Magnetosonic Wave in a Multi-Ion Plasma; June 1995

NIFS-364 H. Sugama and W. Horton
Entropy Production and Onsager Symmetry in Neoclassical Transport Processes of Toroidal Plasmas; July 1995

NIFS-365 K. Itoh, S.-I. Itoh, A. Fukuyama and M. Yagi,
On the Minimum Circulating Power of Steady State Tokamaks; July 1995

NIFS-366 K. Itoh and Sanae-I. Itoh,
The Role of Electric Field in Confinement; July 1995

NIFS-367 F. Xiao and T. Yabe,
A Rational Function Based Scheme for Solving Advection Equation; July 1995

NIFS-368 Y. Takeiri, O. Kaneko, Y. Oka, K. Tsumori, E. Asano, R. Akiyama, T. Kawamoto and T. Kuroda,
Multi-Beamlet Focusing of Intense Negative Ion Beams by Aperture Displacement Technique; Aug. 1995

NIFS-369 A. Ando, Y. Takeiri, O. Kaneko, Y. Oka, K. Tsumori, E. Asano, T. Kawamoto, R. Akiyama and T. Kuroda,
Experiments of an Intense H- Ion Beam Acceleration; Aug. 1995

NIFS-370 M. Sasao, A. Taniike, I. Nomura, M. Wada, H. Yamaoka and M. Sato,
Development of Diagnostic Beams for Alpha Particle Measurement on ITER; Aug. 1995

NIFS-371 S. Yamaguchi, J. Yamamoto and O. Motojima;
A New Cable -in conduit Conductor Magnet with Insulated Strands; Sep. 1995

NIFS-372 H. Miura,
Enstrophy Generation in a Shock-Dominated Turbulence; Sep. 1995

NIFS-373 M. Natsir, A. Sagara, K. Tsuzuki, B. Tsuchiya, Y. Hasegawa, O. Motojima,
Control of Discharge Conditions to Reduce Hydrogen Content in Low Z Films Produced with DC Glow; Sep. 1995

NIFS-374 K. Tsuzuki, M. Natsir, N. Inoue, A. Sagara, N. Noda, O. Motojima, T. Mochizuki, I. Fujita, T. Hino and T. Yamashina,
Behavior of Hydrogen Atoms in Boron Films during H_2 and He Glow Discharge and Thermal Desorption; Sep. 1995

NIFS-375 U. Stroth, M. Murakami, R.A. Dory, H. Yamada, S. Okamura, F. Sano and T.

Obiki,
Energy Confinement Scaling from the International Stellarator Database;
Sep. 1995

NIFS-376 S. Bazdenkov, T. Sato, K. Watanabe and The Complexity Simulation Group,
Multi-Scale Semi-Ideal Magnetohydrodynamics of a Tokamak Plasma;
Sep. 1995

NIFS-377 J. Uramoto,
Extraction of Negative Pionlike Particles from a H2 or D2 Gas Discharge Plasma in Magnetic Field; Sep. 1995

NIFS-378 K. Akaishi,
Theoretical Consideration for the Outgassing Characteristics of an Unbaked Vacuum System; Oct. 1995

NIFS-379 H. Shimazu, S. Machida and M. Tanaka,
Macro-Particle Simulation of Collisionless Parallel Shocks; Oct. 1995

NIFS-380 N. Kondo and Y. Kondoh,
Eigenfunction Spectrum Analysis for Self-organization in Dissipative Solitons; Oct. 1995

NIFS-381 Y. Kondoh, M. Yoshizawa, A. Nakano and T. Yabe,
Self-organization of Two-dimensional Incompressible Viscous Flow in a Friction-free Box; Oct. 1995

NIFS-382 Y.N. Nejoh and H. Sanuki,
The Effects of the Beam and Ion Temperatures on Ion-Acoustic Waves in an Electron Beam-Plasma System; Oct. 1995

NIFS-383 K. Ichiguchi, O. Motojima, K. Yamazaki, N. Nakajima and M. Okamoto
Flexibility of LHD Configuration with Multi-Layer Helical Coils;
Nov. 1995

NIFS-384 D. Biskamp, E. Schwarz and J.F. Drake,
Two-dimensional Electron Magnetohydrodynamic Turbulence; Nov. 1995

NIFS-385 H. Kitabata, T. Hayashi, T. Sato and Complexity Simulation Group,
Impulsive Nature in Collisional Driven Reconnection; Nov. 1995

NIFS-386 Y. Katoh, T. Muroga, A. Kohyama, R.E. Stoller, C. Namba and O. Motojima,
Rate Theory Modeling of Defect Evolution under Cascade Damage Conditions:The Influence of Vacancy-type Cascade Remnants and Application to the Defect Production Chracterization by Microstructural Analysis; Nov. 1995

NIFS-387 K. Araki, S. Yanase and J. Mizushima,
Symmetry Breaking by Differential Rotation and Saddle-node Bifurcation

of the Thermal Convection in a Spherical Shell; Dec. 1995

NIFS-388 V.D. Pustovitov,
Control of Pfirsch-Schlüter Current by External Poloidal Magnetic Field in Conventional Stellarators: Dec. 1995

NIFS-389 K. Akaishi,
On the Outgassing Rate Versus Time Characteristics in the Pump-down of an Unbaked Vacuum System; Dec. 1995

NIFS-390 K.N. Sato, S. Murakami, N. Nakajima, K. Itoh,
Possibility of Simulation Experiments for Fast Particle Physics in Large Helical Device (LHD); Dec. 1995

NIFS-391 W.X.Wang, M. Okamoto, N. Nakajima, S. Murakami and N. Ohyabu,
A Monte Carlo Simulation Model for the Steady-State Plasma in the Scrape-off Layer; Dec. 1995

NIFS-392 Shao-ping Zhu, R. Horiuchi, T. Sato and The Complexity Simulation Group,
Self-organization Process of a Magnetohydrodynamic Plasma in the Presence of Thermal Conduction; Dec. 1995

NIFS-393 M. Ozaki, T. Sato, R. Horiuchi and the Complexity Simulation Group
Electromagnetic Instability and Anomalous Resistivity in a Magnetic Neutral Sheet; Dec. 1995

NIFS-394 K. Itoh, S.-I Itoh, M. Yagi and A. Fukuyama,
Subcritical Excitation of Plasma Turbulence; Jan. 1996

NIFS-395 H. Sugama and M. Okamoto, W. Horton and M. Wakatani,
Transport Processes and Entropy Production in Toroidal Plasmas with Gyrokinetic Eletromagnetic Turbulence; Jan. 1996

NIFS-396 T. Kato, T. Fujiwara and Y. Hanaoka,
X-ray Spectral Analysis of Yohkoh BCS Data on Sep. 6 1992 Flares - Blue Shift Component and Ion Abundances -; Feb. 1996

NIFS-397 H. Kuramoto, N. Hiraki, S. Moriyama, K. Toi, K. Sato, K. Narihara, A. Ejiri, T. Seki and JIPP T-IIU Group,
Measurement of the Poloidal Magnetic Field Profile with High Time Resolution Zeeman Polarimeter in the JIPP T-IIU Tokamak; Feb. 1996

NIFS-398 J.F. Wang, T. Amano, Y. Ogawa, N. Inoue,
Simulation of Burning Plasma Dynamics in ITER; Feb. 1996